View metadata, citation and similar papers at core.ac.uk

brought to you by CORE

provided by Elsevier - Publisher Connector

Available online at www.sciencedirect.com

ScienceDirect

Procedia Engineering 130 (2015) 1162 – 1176

Procedia Engineering

www.elsevier.com/locate/procedia

14th International Conference on Pressure Vessel Technology

Significance and Assessment of Low Temperature Creep and Irradiation Creep in Nuclear Reactor Applications

Y.S. Garud[a,*]

[a]*SIMRAND LLC, 5339 Romford Dr., San Jose, California, U.S.A.*

Abstract

The mechanisms and characteristics of low temperature creep and irradiation creep of structural alloys in light water reactor service are briefly reviewed. The significance of creep is made clear in relation to the environmentally-assisted cracking (EAC). It is shown that while total creep itself may not be significant the attendant slow strain rates are likely contributors critical to the manifestation of EAC. This interrelation of the creep and EAC is further assessed with validation of a continuum damage mechanics approach to quantify the EAC kinetics. Limitations of the formulation and other approaches are discussed, with a note that the influence of irradiation creep on EAC appears not to have been taken into account at present. These aspects are discussed identifying possible useful refinements in assessing the role of creep in EAC.

© 2015 The Authors. Published by Elsevier Ltd. This is an open access article under the CC BY-NC-ND license (http://creativecommons.org/licenses/by-nc-nd/4.0/).

Peer-review under responsibility of the organizing committee of ICPVT-14

Keywords: Low temperature creep; Irradiation creep; Environmentally-assisted Cracking; Strain rate; Damage mechanics; Stress corrosion

1. Background and objective

Creep of a metallic component, as a time-dependent deformation under a set of fixed stress and temperature, has been investigated for at least over a century; its physics and phenomenology have been amply summarized by many [e.g. 1–4]. In service, the creep related deformation typically occurs under variable stress and/or temperature which act to enhance the creep. This deformation and associated strain rates are generally not taken into account in the design of metallic components operating below about 650 K (or about 0.39 on homologous scale), as the creep

* Corresponding author. Tel.: +1-408-266-3033; fax: +1-408-266-3033.
E-mail address: yogen@garud.com

1877-7058 © 2015 The Authors. Published by Elsevier Ltd. This is an open access article under the CC BY-NC-ND license (http://creativecommons.org/licenses/by-nc-nd/4.0/).

Peer-review under responsibility of the organizing committee of ICPVT-14
doi:10.1016/j.proeng.2015.12.284

effects are considered to be insignificant at these temperatures. However, the structural metals and alloys do creep below this temperature down to normal room temperature, which is referred below also as the low temperature creep.

Also, environmental effects on material degradation are typically not included in the design process, in part, due to the designer's lack over operational control or of applicable data. For example, in the case of light water reactor (LWR) systems the possible (accelerating) effects of aqueous corrosion or irradiation on environmentally assisted cracking (EAC) due to cyclic or steady loads are not explicitly addressed in the component design. This poses a question and a need to assess the design adequacy for these effects, especially over long-term operation. The objective of this paper is to examine the potential role of creep at low temperature and/or under irradiation in the material degradation of LWR components due to EAC. The paper also describes a possible approach to quantify the EAC damage based on strain rate considerations, and illustrates its implementation and validation.

From years of investigations by many, it has been well recognized that stress corrosion cracking (SCC), and EAC in general, is a result of the conjoint action of three factors broadly classified as the environment (temperature and chemical characteristics), the material (microstructure), and the stress (deformation mechanics). At the same time, universal acceptance or knowledge of a definitive or detail mechanistic understanding of how this conjoint action results in the damage evolution or (sub-critical) cracking is generally lacking, making it difficult to judge the appropriate balance or relative significance of these three factors for general application. As such, some knowledge of these varied but essential disciplines is a required basis for engineering management and quantitative assessment of this form of damage. An interdisciplinary approach, even if simplified, that has a plausible semi-empirical basis is to be preferred; totally physics based approach has proved to be illusive or too complex for engineering application, while purely empirical or statistical approach becomes quite limited in scope, especially for extending data from laboratory (accelerated) conditions to service conditions, or for meaningful ranking of susceptibility from one set of component/conditions to another.

With the above background, the mechanisms and characteristics of low temperature creep and irradiation creep under normal LWR service conditions are briefly reviewed, followed by a summary assessment for the significance of creep in relation to plausible mechanistic aspects and phenomenological observations of EAC. It is shown that while the total creep deformation itself may not be significant, *per se*, the attendant slow strain rates are likely contributors critical to the manifestation and slow kinetics of the EAC degradation. This role of creep and its interaction with EAC damage are further examined within the framework of a continuum damage mechanics approach used to quantify the kinetics of degradation. Results of implementing the approach, its validation, limitations, and further useful developments are discussed.

2. Creep under low temperature and irradiation

While the low temperature creep of structural metals is fairly well known in the scientific/research communities, its effect is typically excluded from design considerations (below about 650 K in the case of steels and nickel-based alloys used in LWR applications). This exclusion may likely have contributed to the belief, at least in the engineering community in general, that the structural metals hardly, if at all, creep in the low temperature regime. As such, a brief review of pertinent creep observations is considered useful as a backdrop for the inclusion of creep below in the assessment of EAC; this review is meant to be illustrative rather than being exhaustive. A more recent review of data and related mechanisms of creep [5] also provide a confirmation of the low temperature creep of several structural metals.

For instance, in one of the early works [6] creep was measured under direct stress in a number of metals, including copper, aluminum, steel, and monel metal, where it was noted that (a) very small but definite amount of creep occurred even at very low stresses at room temperature, and (b) the creep continued for indefinitely long period, specimens having found to continue to deform after six years. Likewise, long-term (beyond 10,000 hours) creep at room temperature, even below yield stress levels, was reported on standard 18-8 stainless steel [7], and beyond 2400 hours at room temperature in AISI Type 347 steel near yield stress [8]. Significant post-yield creep strains were reported in mild steel and in austenitic stainless steels even at room temperature [9, 10]; also, creep within the plastic enclave at a notch was noted in an otherwise elastically deforming member and the creep behavior paralleled that of the post-yield unnotched member [10]. The occurrence of creep in Alloy 600 around 633 K was experimentally confirmed [11] also concluding that the creep plays an important role in the intergranular SCC

observed in Alloy 600 in high purity water. The creep of several related nickel base alloys in the low temperature regime was summarized in [12]. Similar creep observations have been confirmed in other austenitic/ferritic steels [13] and in high strength steels [14].

In general, the low temperature, low stress creep is classified as the logarithmic or primary creep where the strain rate typically falls with time due to the material hardening related to the increased resistance to dislocation glide that may be overcome with the thermally activated cross-slip process, especially in face-centered cubic alloys, dependent on the stress level. At somewhat higher temperatures the vacancy related and diffusion based mechanisms become more significant as well. Under service conditions, operational load fluctuations and the trend towards use of load-following act as an added source of strain rate due to possible re-starting of the primary phase in which the creep rate is usually enhanced compared to that at the steady state. Furthermore, local interaction and damage due to environmental effects act to sustain or accelerate the local inelastic deformation response.

Several LWR vessel internal components, even though operating below about 650 K, are also subject to irradiation, in addition to the stress and temperature conditions, which leads to material damage over time that is cumulative in nature. The inelastic and time dependent deformation is enhanced under the simultaneous action of stress and irradiation, and it is called the irradiation creep[1] that is distinct and distinguished from the commonly known thermal creep. It is another source of time-dependent straining in reactor internals, in addition to the other sources of creep noted above. This enhanced inelastic deformation is a result of the continuing material damage caused by the bombardment of high energy (about 0.1 to 1 MeV and above) neutrons that produce excess vacancies, interstitials, their faulted or prismatic loops, and stacking-fault tetrahedra [16–18], which, in turn, interact and influence the glide and climb motion of dislocations. The effect of irradiation damage on material creep, often attributed to these induced defects, has been reported for many years [e.g., 19, 20] as a straining mechanism separate from thermal creep, although its impact on thermally activated mechanisms can't be completely excluded especially at higher range of temperature and/or stresses. The irradiation creep has often been examined or closely associated with the void swelling phenomenon under irradiation at mid-to-high temperatures, although the two are distinct.

Under the typical conditions of LWR operation the strain rate contribution due to irradiation can be significant in comparison with the thermal creep, where the former is weakly dependent on temperature and has a much lower sensitivity to stress; several reviews cover the relevant experimental observations [e.g., 19–21]. Experimental work has also confirmed irradiation creep in the case of 300-series stainless steels [22] under LWR conditions. The underlying mechanisms still involve interaction effects of stress with dislocation motion of glide/climb and vacancies, but continuing especially below yield stress with nearly linear dependence of strain rate on stress and on the irradiation (neutron) flux. Due to the irradiation induced defects the mechanism of dislocation climb is operative even at the lower temperatures as well, leading to the climb-assisted/enhanced glide of dislocations as a possible mechanism [23]. Indeed, based on a dislocation climb model for the steady-state irradiation creep of non-fissile materials at low-temperature, the linear dependence of creep rate on applied stress and on irradiation flux, independent of temperature, was predicted [24, 25] and experimentally observed [25, 26]. Also, various mechanisms of irradiation creep as reviewed [27, 28] emphasize the involvement of dislocation processes and their interaction with other defects under stress. These mechanisms include the so-called stress-induced preferential absorption (SIPA) of interstitials at edge dislocations, the stress-induced preferred nucleation (SIPN) of dislocation loops, climb-enabled preferred-absorption glide (PAG) [29], and the radiation and stress induced difference in emission (RSIDE) of vacancies from dislocations of different orientations with respect to the external stress [30].

It is concluded that the metallic materials are subject to measurable creep deformation even under conditions of relatively low temperatures and stresses in LWR service, with or without irradiation. Although the significance of this creep may be little with regard to the component strength or total deformational considerations, this is not necessarily the case with respect to the EAC damage, especially over long periods of operation, due to the resulting slow and sustained strain rates, as discussed below.

---

[1] As a note of historic interest, one of the earliest (if not the first) findings on the effect of irradiation on creep were reported by Andrade, in 1945 [15], whose name is famously associated with the primary creep law for unirradiated metals.

3. Significance of creep in EAC

Creep is an active form of straining that contributes to relatively slow strain rates at low temperatures/stresses. Higher or changing stress/thermal conditions enhance the viscous and non-viscous (elastic-plastic) strain rates. Even if one considers the stress–temperature regime dominated by the typical primary creep response, the cyclic conditions can re-initiate the primary creep; also, any form active material damage—such as due to the interaction of environment and its interface with the material—will enhance local straining as well. The net resultant and continued straining has been considered to play a critical role in the process of EAC [e.g., 31–36], and it has led to a standard practice for slow strain-rate testing [37]. The significance of strain rate, including creep, was also made more explicit in the earlier quantitative modeling of SCC response of Type 304 stainless steel in oxygenated water [38] and of Ni-Cr-Fe Alloy 600 in de-oxygenated water [39] typical of LWR conditions. This role of strain rate, as briefly discussed below, is supported by phenomenological and service failure observations, as well as plausible mechanistic considerations.

In many alloy–environment systems the range of parameters for EAC susceptibility typically coincides with (a) excellent resistance to general corrosion, in the absence of any stress, and (b) the electrochemical corrosion potential region where the corrosion current density is highly sensitive to changes in the potential. This is especially the case for normally ductile materials such as the austenitic stainless steels and nickel base alloys in LWR type aqueous environments. This common phenomenological observation alone suggests the nature of interaction for EAC to involve a protective interface (a corrosion product or an oxide film) and its repeated local disruption (or degradation in protective quality) particularly due to the mechanical straining action.

Experimentally, for example, with a series of discriminating tests it was demonstrated that creep deformation and strain rate, rather than stress *per se*, were responsible for the manifestation of SCC in Alloy 600 tubing under primary water environment [40]; similar results were reported in other systems [34]. Several characteristics and influences of SCC have been commonly observed to display strong correlation or dependence on the applied strain rate: e.g., with lowering strain rate, the peak stress and failure strain in a tensile test are reduced while the percent area affected by SCC damage is increased; the failure time and average SCC penetration rate also show correlation with the strain rate. Example case studies in LWR water environments include SCC data on Type 304 stainless steels [41] and on Ni-Cr-Fe Alloy 600 [42].

Additionally, a more critical comparison between the effect of stress, *per se*, versus the significance of applied strain rate is illustrated in Fig. 1 using data from SCC of Alloy 600 in high purity water [42–44]: here the dashed line is a re-potted stress–time history in a constant extension rate test (CERT) at 638 K with $3x10^{-7}$ s^{-1} strain rate; the symbols are failure times obtained at various fixed applied stress levels for the same heat of Alloy 600 also tested at 638 K; and *Sy* denotes the corresponding room temperature yield strength. The comparison shows that the failure time is much reduced in CERT despite the fact that the time is spent at relatively low stress levels at which the constant load tests survived for much longer periods. Similar conclusion also can be reached, for example, in the case of intergranular SCC of Type 304 stainless steel in BWR type oxygenated water, by comparing stress versus time response in CERT [45] with that in constant load tests [46].

Furthermore, the significance of creep (at 633 K) as a source of the strain rate was also suggested by correlating the effect of compositional variations on the SCC susceptibility of Alloy 600 type materials with a parallel effect on their creep response [47, 48], including the role of mechanical creep damage depending on the loading severity and accumulated intergranular damage [49]. The accelerating influence of slow strain rates under CERT even in the normally SCC-resistant Alloy 690 was recently confirmed [50] indicating that, for a given uniform strain applied, the SCC degradation was greater at slower strain rates and that the time-dependent component of the environmental interaction was enhanced, especially in the initiation phase of the damage. The importance of slow straining action in SCC has also been confirmed in several other material–environment systems [e.g., 51–54], in addition to the Ni-base alloys and 300-series austenitic steels in LWR environments.

As an example of actual service related SCC failures in a given set of Alloy 600 tubing material and primary water environment, it may be noted that the earliest such failures were found in the U-bend region of these tubes which were subject to the so-called denting (i.e., continued squeezing of the two legs of a U-bend) [55] which is a form of active straining imposed in addition to the service temperature and pressure loads — other regions in the same system of tubing and environment, including those with somewhat higher temperatures than at the U-bends,

did not show the SCC until much later, if at all. Another early service related experience to note is that of the extensive cracking in fuel rod cladding made of Type 304 stainless steel in LWR environments [e.g., 56]. The defects developed as a result of irradiation-assisted stress corrosion cracking (IASCC) at specific locations in any given fuel rod subject to the same environment and in a material condition that did not show any grain boundary carbides/sensitization; also the cracking was observed in initially annealed as well as cold-worked conditions. The specific locations of cracking were confined to high levels of stress and irradiation, and where high localized inelastic deformation was occurring at fuel pellet interfaces due to the pellet–to–clad interaction during irradiation. These case studies are noted as examples discriminating the critical role of active straining relative to other factors in SCC and IASCC.

As such, the significance of strain rate as a key variable in SCC, and in EAC in general, is strongly in accord with the above phenomenological observations and mechanistic considerations pertinent to the manifestation of SCC. It is to be noted that in terms of the film rupture (or interface disruption) mechanism underlying the SCC/EAC damage, the important aspect is the balancing action (or relative rates) of the processes of mechanical disruption governed by the deformation mechanics and the formation of protective interface layer governed by the environmental (electrochemical) influence; this aspect is taken into account in quantifying the damage as described below in which the actual details of the two processes need not be specified beyond a semi-empiric approach. The additional practical benefit of explicitly relating the strain rate parameter to damage is that it provides a consistent and unifying basis for interpreting and correlating the SCC/EAC damage under widely differing loading conditions in laboratory tests and under service conditions.

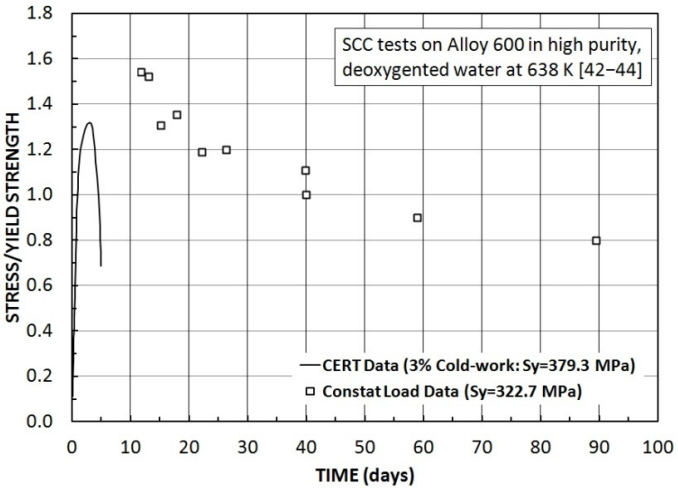

Fig. 1. Comparison of stress levels and failure response under CERT and constant load tests, illustrating significance of strain rate versus stress.

4. Damage mechanics approach

Having established the significance of strain rate as a key driver in relation to the development of EAC damage, it is of interest to examine the possible quantification of this damage by integrating the deformation mechanics, including creep, and the expected corrosion kinetics for a given material–environment system. In order to address the role of deformation process more explicitly, it is clear that some form of material constitutive relations should be an essential part of an EAC model and that the constitutive relations should include the time dependent straining response. Furthermore, the progression of damage, in this case due to the environmental effects, should be related to the straining as well. With progressive damage, it is to be expected that the load bearing net section area will decrease leading to increasing local stress and strains relative to their nominal values. Also, due to the localized nature of interaction at the interface between the environment and the material, the rate of damage is expected to

influence the effective straining within the local damage zone; this influence should be addressed in considering the relative rates, or balancing, between the local deformational and environmental damage processes. If the local deformation is too fast or too slow for the environmental influence to manifest then the EAC damage process should subside, but continue otherwise.

The above characteristics of EAC and their integration can be summarized by the logic shown in Fig. 2. (In this figure the boxes with rounded corners are inputs, those with bold rectangle are points of calculation, and those with questions are logical comparisons). The figure incorporates three functional relations denoted by *(D), (F), and (G)*:

(D) is the accumulated EAC damage that may be related to the effective depth of penetration (or loss of load-bearing area).
(F) represents the corrosion–deformation interaction relating the local damage rate, $\dot{D}$, and the effective strain rate, $\dot{\varepsilon}$.
(G) denotes the local stress–strain response incorporating the influences of effective local stress σ and the rate of damage on the effective strain rate, where σ is dependent on the extent of damage, D.

The major computational steps in the above logic can be summarized as follows.

1) The nominal stress and strain (i.e., in the absence of any damage) are determined from the loading condition, component or specimen geometry, and the material constitutive relations.
2) The effective local stress is related to the nominal stress, the accumulated damage (D) and its growth rate at the time that is incrementally changed, if the section did not reach the applicable failure criterion.
3) The effective local strain rate is estimated based on the effective stress (and the material constitutive relations), the accumulated damage, and current SCC damage growth rate. The local strain rate is compared with a specified set of upper and lower critical values for the damage to manifest
4) A functional relation (F) between the SCC damage rate and the local strain rate is used to determine the current damage rate; this relation is specified in terms of the SCC parameters dependent on the material (condition) and the environment, including temperature. (In Fig. 2, the dashed arrow connecting the failure box and the material–environment box is to account for the possible change in this combination, although in this paper the material and environment are fixed with respect to time or damage accumulation.)

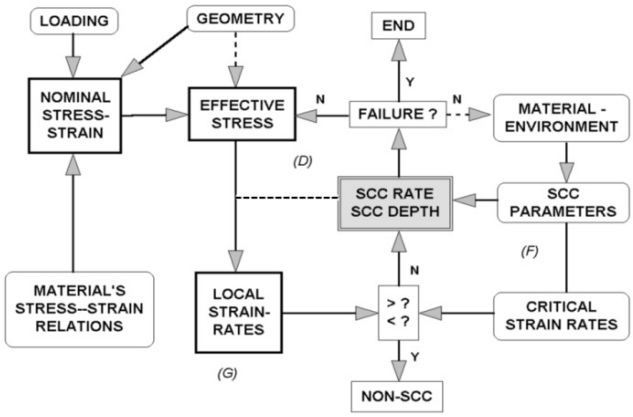

Fig. 2. Logic for the strain-rate damage mechanics approach to assess corrosion-deformation interaction in SCC.

Analytically, the resulting damage mechanics formulation can be described by the following generic expressions:

$$\dot{D} = F\left[\dot{\varepsilon}, D, T\right] \tag{1}$$

$$\dot{\varepsilon} = G\left[\sigma, D, \dot{D}, T\right] \tag{2}$$

$$\dot{\sigma} = g_1\left[D\right]\cdot\dot{\sigma}_{nom} + g_2\left[D\right]\cdot\sigma_{nom}\cdot\dot{D} \tag{3}$$

Here, T is the applicable temperature, the subscript "*nom*" is used to denote the corresponding nominal value (i.e., in the absence of any damage), and g_1 and g_2 are the geometry dependent functions of damage, D, relating the nominal and local (effective) stresses. The function G depends on the specified material constitutive relations. The above formulation is referred to as the strain rate damage mechanics (SRDM) approach. This may be viewed essentially as an extension of the continuum damage mechanics approach [1] used in quantifying creep damage (usually at high temperatures), to include the damage due to the environmental effects in SCC/EAC.

Ideally, the function F (Equation 1) should be obtained from first principles in the applicable material–environment system of interest; however, for the purpose of an engineering model, it is deemed sufficient to assume a reasonable form for this with verification for internal consistency and expected trends from the relevant data. The choice of material constitutive relations to describe the function G (Equation 2) is guided by the available data and desired physical basis or general applicability for a given set of material(s)/conditions of interest. The specific functions and respective parameters used in the implementation discussed in this paper are summarized in the *Appendix*. The above logic is implemented with the set of equations integrated numerically using suitable time increments to compute the cumulative damage.

5. SRDM results

The above SRDM approach and its validity are illustrated here with its implementation for two types of loading commonly used in evaluating the SCC susceptibility in a given material–environment combination. One is the constant extension rate test (CERT) in which active, nearly fixed (nominal), known strain rate is imposed to maintain an accelerated kinetics of SCC. The other is the constant load test, with fixed (nominal) stress, in which the strain rate contribution is primarily due to the time dependent deformation from material creep and local damage response. In particular, the data from CERT are used here to determine the SRDM parameters, and the SCC response under constant load condition is predicted with the SRDM model; the predicted SCC response is then compared with the data from constant load tests.

To reduce any impact of heat-to-heat variability in this assessment, all data are taken from a single heat of material – a mill-annealed condition of Ni-Cr-Fe Alloy 600 with 0.01% carbon content [42–44]. This material is fairly susceptible to IGSCC in high purity, deoxygenated water: the reported test environment had very low conductivity and dissolved oxygen less than 5 ppb. The CERT data were reported over the temperature range of 563 K to 638 K, and the constant load tests were carried at 638 K. The tests were conducted on typical plate type (6.35 mm wide, 25.4 mm gauge length) tensile specimens cut from tubing of about 1.53 mm thickness. The CERT samples had an initial cold-work of about 3% due to flattened split tubing [42]; the constant load specimens were cut from the as-received tubing but without flattening or rolling [43, 44]. For reference, the CERT data are summarized below in Table 1.

The material constitutive relations in this work use the Bodner-Partom formulation [58] as described in the *Appendix* that also lists the respective parameters for the as-received and cold-worked conditions. The nominal and local stress–strain quantities were related through the effective stress based on the net-section using the flat plate geometry functions given in the *Appendix*. The corrosion–deformation interaction function F given in the *Appendix* (Equation A.1, with Q = 138.2 kJ/mol and ϕ = 0.5) is used with its parameter α_0 that was estimated to provide a reasonable fit to test data from three CERTs (#2, #6, and #7 in Table 1) for which clear stress–strain response was also available.

Table 1. Data from constant extension rate tests on Alloy 600 tubing, heat #4, in high purity, deoxygenated water [42].

Test No.	Temperature K	Strain rate 1/s	SCC depth mm	SCC rate mm/s	SCC period* days	Peak true stress^ MPa
1	563	5.00E-08	0.15	2.87E-08	60.5	–
2	598	3.90E-08	0.95	4.44E-07	24.8	520.3
3	598	4.95E-08	1.33	4.98E-07	30.9	–
4	598	2.90E-07	0.40	3.31E-07	14.0	–
5	618	2.70E-07	1.29	1.58E-06	9.4	–
6	618	3.00E-07	0.80	1.35E-06	6.9	604.1
7	638	2.60E-07	1.15	2.60E-06	5.1	464.1

* SCC period is equal to the reported depth divided by IGSCC rate.
^ Peak true stress estimated from the stress-strain curves.

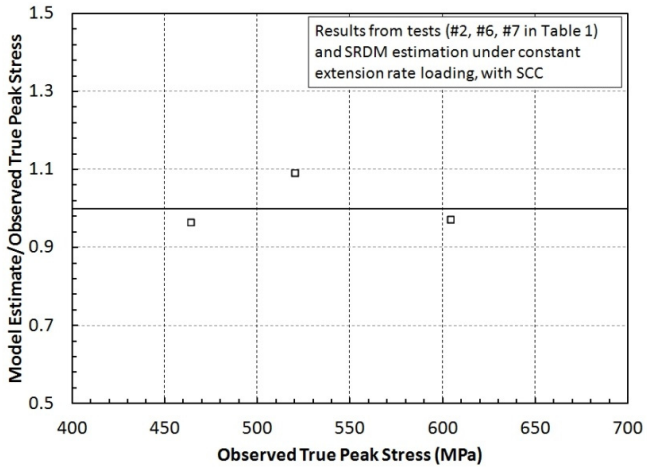

Fig. 3. Comparison of SRDM model fit with reported peak true stresses for three constant extension rate tests.

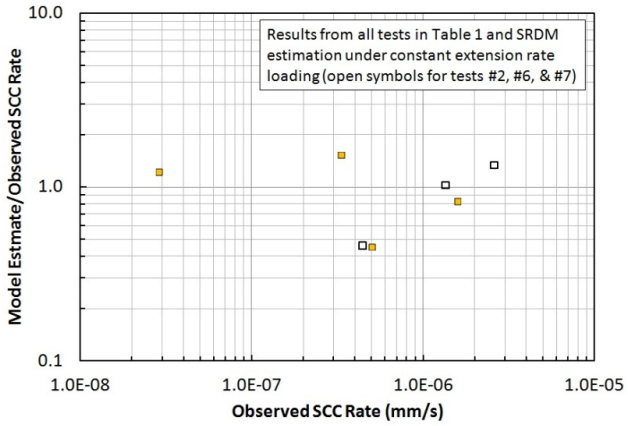

Fig. 4. Comparison of SRDM estimates of SCC failure periods with reported data for all constant extension rate test conditions listed in Table 1.

In particular, the reported data on the time of active SCC penetration, and the true peak stress reached (listed in the last two columns of Table 1) in each of these three tests were compared with the SRDM estimates to obtain the value of α_0. The best-fit value of α_0 = 356 km/s resulted in model estimates of the SCC time to within a factor of two of the data. The model estimates of true peak stresses were within 10% of the reported data values, as shown in Fig. 3. Data for other CERTs in Table 1 were compared with the SRDM results for consistency and model verification. Fig. 4 illustrates this comparison for all Table1 tests which shows the model estimates for the average rate of SCC penetration to be within a factor of about two on the observed rates; note that the penetration rates data were not used in the determining the value of α_0. As such, the model is considered to be consistent and in reasonably good agreement with the CERT results.

SCC data were also reported for several constant load conditions [43, 44] for the same environment and specimen geometry as used in the above assessed CERTs. The applied loads covered a wide range of the fixed nominal stress – from about 80% to 154% of the material yield strength (322.7 MPa at room temperature). These tests were done at 638 K temperature using the same heat of Alloy 600; however, as noted earlier, the material was in the as-received condition as compared to the cold-worked condition (379 MPa yield strength) of the CERT samples. The SCC response is known to be sensitive to the cold-work level and related high strength [59, 60]; from the assessment of their CERT data it was reported that the average rate of SCC kinetics in cold-worked condition was about 2.5 times faster than that for the non-flattened, as-received condition [61, 62]. Therefore, the above estimate of α_0 was reduced by this factor, to 142 km/s, in analyzing the constant load SCC data. The SRDM formulation was used to predict the SCC failure times for various fixed nominal stress conditions, with the above SCC parameters derived from the CERT data and the constitutive model parameters given in Table A-1 for the as-received Alloy 600 condition. These predicted SCC failure times are compared with the reported data as shown in Fig. 5, where the solid line shows the predicted stress dependence, at 638 K. The comparison shows that the observed failure times are mostly within a factor of 1.5 (shown by the two dashed lines in Fig. 5) of the prediction. Given that none of the test data shown in Fig. 5 was used in the SRDM assessment of these constant load tests, the predicted stress dependence is judged to be acceptable and a reasonable validation of the SRDM approach.

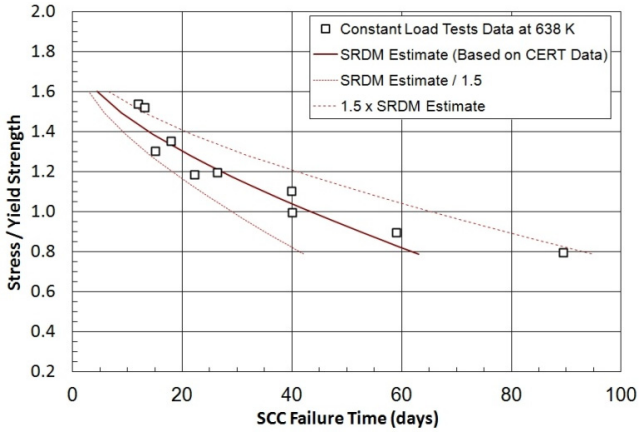

Fig. 5. Comparison of SRDM predicted response of SCC failure times with data [43, 44] under constant load conditions.

6. Discussion

The above results using the SRDM logic demonstrate that the strain rate basis offers a unified treatment of different types of loading conditions, including accelerated tests, and confirm the validity of the approach consistent with major trends with regard to the SCC susceptibility, as well as the plausible mechanistic considerations, although the approach is semi-empirical. The key elements of the approach can be related to or interpreted in terms of the repeated interruption of otherwise protective nature of the interface between the environment and the material

caused by the deformation process, while implicitly accounting for the local development of damage. In this regard, although the detailed mechanistic understanding is not yet clear or complete, the slow straining and localized deformation have been implicated even when hydrogen influence may be involved in EAC [53, 63, 64]; as such, this influence is accounted for, at least in principle, in the semi-empiric strain-rate based damage evaluation approach.

It is interesting to note that the use of damage-based effective stress concept in the framework of continuum damage mechanics, similar to that discussed in this paper and in [57], was also shown to be in agreement with data in modeling the SCC response of Type 304 stainless steel in acid chloride solution in another study [65]—albeit with a different constitutive model noted to have a thermodynamic basis.

To a first approximation, the effective stress in the present application of SRDM was equated to the net-section stress—this is neither a requirement nor a limitation of the formulation. The basis equations are flexible enough to incorporate further non-linear damage for local interaction or environmental effects, if required, by modifying the effective stress to be more sensitive to the local damage accumulation. Alternatively, an enhancement to the current formulation is considered more effective if an additional state variable is introduced to reflect the local strength reduction due to environmental interaction.

The continuum damage approach discussed in this work does not require a pre-existing crack to be present or environmental conditions to be fixed for its application. It is often considered, however, that a well-defined singular crack is present and that its growth kinetics should in principle, if not in strict sense, be related to the strain-rate at the crack-tip. Considering that the mechanical strain, by definition, refers to the gradient of displacement of nearing physical points, the strain rate at crack-tip is difficult to define, let alone estimate, more so at the tip of a growing crack. An alternative treatment of SCC kinetics is then often based on fracture mechanics type specimens with large initially cracked geometries, and utilizes some form of crack-tip strain rate estimation [e.g., 66] that necessarily introduces empiricism and additional parameters. The use of linear elastic fracture mechanics (LEFM), at least for assessing the crack growth rate of a defined crack, is fairly common in addressing the EAC, and deserves a brief comment. LEFM describes the linear elastic stress–strain fields surrounding, but not at, the tip of a well-defined singular crack under static conditions, and uses the LEFM type parameters to relate these fields to the remote (nominal) stress conditions on the basis of a similitude argument, for an idealized linear elastic material behavior disregarding any changes and features in the microstructure. Further, under EAC conditions, there is a fundamental loss of the similitude due to the significant, possibly intense, interaction between the electrochemical (corrosion) and thermo-mechanical (deformation) processes responsible for the EAC kinetics. That is, the crack driving force, *per se*, is not only mechanical but electrochemical, and the two do not have the same dependence or scaling with geometry. Also, material constitutive relations for any time dependence or damage dependence are not considered in such an approach. These limitations render this alternative to EAC assessment to be necessarily empirical in nature.

In this paper, the implementation of SRDM used for demonstration and validation of the approach to quantify the SCC damage was limited to unirradiated conditions, although the significance of irradiation creep and its relation to IASCC were also discussed. Considering the common understanding that IASCC and SCC share the same mechanism(s) it is reasonable to expect that the presented approach should also be applicable to assess the IASCC damage. This application needs to be further developed as a useful extension of the SRDM basis, addressing the possible effect of additional creep with its dependencies on the irradiation flux/fluence and stress as noted earlier in the paper. Further assessment would be useful to ascertain whether appropriately modified constitutive relations to account for the effect of irradiation on strain rate, would adequately capture the enhancement in SCC kinetics, or changes to the damage rate relation (Equation A.1, in particular the parameter α_0) would also be required; this can be done with parametric evaluation and comparison with IASCC test data. Obviously, the framework and methodology as described here can be utilized for this assessment and it can thus be seen also to enable evaluation of the relative contribution or sensitivity of deformation mechanics parameters vis-à-vis those of the environmental influence.

7. Summary and conclusions

In this paper the occurrence and characteristics of low temperature creep and irradiation creep under LWR service conditions were reviewed. From this review it was concluded that the metallic materials are subject to measurable creep deformation even under conditions of relatively low temperatures and stresses, with or without irradiation. The total creep may not be too large to affect the strength and deformation limits for operation; however,

the resulting slow and sustained strain rates over long periods of operation are likely to be significant with respect to the EAC damage accumulation.

The significance of strain rate and its relation to plausible EAC damage mechanisms were examined, and this role of strain rate was supported with a brief but critical assessment of several phenomenological and service failure observations.

An approach to account for the material deformation and its interaction with the corrosion process was summarized using the framework of damage mechanics in which strain rate and EAC damage rate processes are coupled. In this approach the material deformation response utilizes inelastic constitutive relations with integration of a damage function representing the interactive nature of the EAC process.

The logic and computational steps for implementing the approach were described and illustrated with its implementation for two types of loading commonly used in evaluating the SCC susceptibility in a given material–environment combination, with differing strain rate characteristics: a constant extension rate test and a constant load test. The SCC data from constant extension rate tests were used to determine the parameters of damage function which showed internal consistency and reasonably good agreement between the data and model estimations for SCC life and peak stress in these tests.

The damage mechanics formulation was validated with the failure times for a range of constant load tests as predicted by using the parameters that were based on the independent data from the constant extension rate tests, using the same heat of material and environmental conditions. Good agreement was found between the predicted results of stress dependence and failure times and SCC data for the constant load conditions.

Limitations of the damage mechanics formulation and other bases in quantifying the EAC response were briefly noted. Also, from the review of literature it was noted that the influence of irradiation creep on EAC appears not to have been made explicit or taken into account at present. These aspects were discussed identifying possible useful refinements to the strain rate based assessment of EAC damage. It is reasonable to expect that the presented approach should also be applicable to assess the IASCC damage and that it needs to be further developed as a useful extension of the SRDM basis, addressing the possible effect of additional damage due to effects of irradiation.

Appendix A.

A.1. SCC kinetics

SCC continues to be one of the active degradation mechanisms in several safety related components of nuclear reactor systems, requiring engineering assessment and adequate management, especially for long term operations. Two of the prominent cases of SCC investigated in these systems include the intergranular stress corrosion cracking (IGSCC) of austenitic (300-series) stainless steels in boiling water reactors (piping, nozzles, and welds), and the primary water stress corrosion cracking (PWSCC) of Ni-Cr-Fe Alloy 600 (tubing, nozzles, and welds) in pressurized water reactors. Both are SCC with intergranular morphology, with respective high purity water environments in the normal operating temperature range of about 555 K to 640 K. In these cases the temperature dependence of SCC kinetics is generally accepted to follow the Arrhenius (exponential) form, and earlier research [36, 38, and 57] suggested a simple power law for its strain rate dependence; these were found to be adequate in the application of SRDM approach for engineering purposes. The resulting expression used in this work for the damage rate, $\dot{D}$ (Equation 1 in the main text), is given as follows:

$$\dot{D} = \alpha_0 \cdot exp\left(-Q / RT\right) \cdot \dot{\epsilon}^{\phi} \tag{A.1}$$

Here, R is the universal gas constant, 8.314 J/(mol·K), T is the temperature (in absolute scale), Q is the activation energy, and α_0 (the pre-multiplier) and ϕ (the exponent) are material–environment dependent parameters.

The SCC data from constant extension rate tests (CERTs) on Alloy 600 tubing heat tested in high purity water [62] provided an estimate of 138.2 kJ/mol for the activation energy. This value is in the range of apparent activation energy of about 126 to 147 kJ/mol reported for similar conditions [43, 44, 61, and 62]; these reports also noted that

the activation energy did not show discernible effect of cold-work. Therefore, the value of Q was taken to be 138.2 kJ/mol, for both the CERTs and the constant load tests analyzed in this work. The value of exponent ϕ was fixed at 0.5 based on a previous initial parametric study using similar SRDM implementation [57]. It is interesting to note from an independent study with a mechanistic interpretation of SCC kinetics in face-centered cubic alloys and its relation to strain rate, that a similar power-law was suggested with the exponent to be in the range of 0.4 to 0.7 for intergranular morphology [67]. The value of α_0 was determined to best-fit the CERT data as described in the *Results* section of the main text; this value was 356 km/s for the 3% cold-work condition of the Alloy 600 tubing used in the CERTs, with the strain rate expressed in units of 1/s.

A.2. Constitutive relations

The constitutive relations to describe the material deformation response in this work are based on the Bodner–Partom formulation [58]; these are used to relate the loading and geometry to the stress–strain and strain-rate history including time-dependent strains. The use of this formulation was guided by the available data for Alloy 600 and its generality to address different types of loading and creep regime of interest [39]; also, it has strong links to the basic microstructural processes underlying the time-dependent deformation response such as the dislocation dynamics, solute strengthening, and related strain hardening/recovery [58]. The formulation utilizes a scalar variable called the "hardness" viewed as an internal variable related to the work of inelastic deformation during the prior load-history; it is summarized by the following relations:

$$\dot{\epsilon} = \dot{\sigma} / E + \dot{\epsilon}_n \;\; or \;\; \dot{\sigma} = E \cdot \left(\dot{\epsilon} - \dot{\epsilon}_n \right) \tag{A.2}$$

$$\dot{\epsilon}_n = \left(2D_0 \Big/ \sqrt{3} \right) \cdot exp\left[-0.5 \left(Z/\sigma \right)^{2n} \right] \tag{A.3}$$

$$\dot{Z} = m \left(Z_1 - Z \right) \cdot \dot{W}_p \tag{A.4}$$

$$\dot{W}_p = \sigma \cdot \dot{\epsilon}_n \tag{A.5}$$

Here, overhead dot denotes the respective rate, σ is the stress, ϵ is the total strain, ϵ_n is the non-elastic strain, W_p and Z represent the state variables for the deformation work density and hardness measure, respectively, and E is the Young's modulus of elasticity; D_0 and Z_1 are material parameters independent of temperature, m and n are material parameters with temperature dependence given by [39]: $m = C_0 + m_0 \cdot T$ and $n = a/T$.

The material specific parameters for two conditions of Alloy 600 used in this work are listed in Table A-1.

Table A-1. Material parameters in the Bodner-Partom constitutive relations of visco-plasticity for two Alloy 600 conditions.

Parameter	Units	As-received	Cold-worked
D_0	1/s	10	10
Z_1	MPa	853	911
a	K	3050	3350
m_0	1/MPa.K	1.897E-05	1.805E-05
C_0	1/MPa	1.115E-02	1.025E-02
m_1	1/K	1.127E-04	1.277E-04
C_1	–	4.798E-01	5.107E-01

The Young's modulus of elasticity is estimated as: $E\ (MPa) = 259363 - 199.244T + 0.205857T^2 + 5.91521x10^{-5}T^3 - 2.029x10^{-7}T^4$, and the initial value of $Z\ (MPa) = (C_1 - m_1\ T)\ Z_1$, based on the assessment of tensile stress–strain data on Alloy 600 [39].

The above constitutive relations are assumed applicable for the nominal (undamaged) section quantities, denoted with the subscript "*nom*", and for the effective (local) section quantities where maximum loss of cross-section due to SCC is occurring.

A.3. Effective stress–strain

Without loss of generality, the cumulative damage D is interpreted to be uniquely related to the depth of SCC penetration. For the flat plate type tensile specimen of thickness h, assuming the SCC penetration to be uniform from both sides across its width, the percent area affected by SCC is also proportional to the peak uniform depth and it is given by $100x(2D/h)$. As such, from simple static equilibrium consideration, the effective stress in the damaged section is related to the nominal stress by the following relation:

$$\sigma = \sigma_{nom} \big/ \left(1 - 2D / h\right) \tag{A.6}$$

From which it follows that the two geometric functions (of Equation 3 in the main text) are given by:

$$g_1\left[D\right] = 1 \big/ \left(1 - 2D / h\right) \tag{A.7}$$

$$g_2\left[D\right] = \left(2 / h\right) \big/ \left(1 - 2D / h\right)^2 \tag{A.8}$$

References

[1] Yu. N. Rabotnov, Creep Problems in Structural Members, American Elsevier Publishing Company, Inc., New York, NY, 1969.
[2] F. R. N. Nabarro, H. L. de Villiers, The Physics of Creep, Taylor & Francis Inc., Bristol, PA, 1995.
[3] M. E. Kassner, Fundamentals of Creep in Metals and Alloys, 2nd ed., Elsevier, Amsterdam, The Netherlands, 2009.
[4] T. H. Hyde, W. Sun, C. J. Hyde, Applied Creep Mechanics, McGraw-Hill Education, New York, NY, 2014.
[5] M. E. Kassner, K. Smith, Review article: Low temperature creep plasticity, Journal of Materials Research and Technology, 3 (2014) 280–288.
[6] R. G. Sturm, in Discussion of: The creep of metals, Applied Mechanics, Paper APM-55-10, Transactions of the ASME, 55 (1933) 61–62.
[7] S. Terai, Creep of 18–8 stainless steel at room temperature, Journal of the Society of Materials Science (Japan), 8 (1959) 652–657.
[8] H. Spahn, in Discussion to paper: Reaction films, metal dissolution, and stress corrosion cracking, by D. A. Vermilyea, in: Fundamental Aspects of Stress Corrosion Cracking, Eds.: R. W. Staehle, A. J. Forty, and D. van Rooyen, NACE, Houston, 1969, pp. 15–31.
[9] D. Kujawski, V. Kallianpur, E. Krempl, An experimental study of uniaxial creep, cyclic creep and relaxation of AISI Type 304 stainless steel at room temperature, Journal of the Mechanics and Physics of Solids, 28 (1980) 129–148.
[10] E. H. Jordan, A. D. Freed, Room-temperature post-yield creep, Experimental Mechanics, 22 (1982) 354–360.
[11] J. K. Sung, G. S. Was, Intergranular cracking of Ni-16Cr-9Fe alloys in high temperature water, Corrosion, 47 (1991) 824–834.
[12] Y. Yi, et al., Creep of nickel alloys in high temperature water, in: Proceedings of the 9th International Symposium on Environmental Degradation of Materials in Nuclear Power Systems – Water Reactors, Eds.: S. Breummer, P. Ford, and G. Was, The Minerals, Metals and Materials Society, Warrendale, PA, 1999, pp. 269–276.
[13] M. M. Festen, J. G. Erlings, R. A. Fransz, Low-temperature creep of austenitic-ferritic and fully austenitic stainless steels and a ferritic pipeline steel, in: Environmental-Induced Cracking of Metals, Eds.: R. P. Gangloff and M. Brian Ives, National Association of Corrosion Engineers, NACE, Houston, TX, 1990, pp. 229–232.
[14] A. Oehlert, A. Atrens, Room temperature creep of high strength steels, Acta Metallurgica et Materialia, 42 (1994) 1493–1508.
[15] E. N. da C. Andrade, Effect of alpha-ray bombardment on glide in metal single crystals, Nature, 156 (1945) 113–114.
[16] R. E. Stoller, Primary Radiation Damage Formation, Section 1.11 in: Comprehensive Nuclear Materials, Volume 1, Ed.: R. J. M. Konings, Elsevier, Amsterdam, 2012, pp. 293–332.
[17] H. Trinkaus, B. N. Singh, C. H. Woo, Defect accumulation under cascade damage conditions, Journal of Nuclear Materials, 212–215 – P1 (1994) 18–28.
[18] B. N. Singh, et al., Review: Evolution of stacking fault tetrahedra and its role in defect accumulation under cascade damage conditions, Journal of Nuclear Materials, 328 (2004) 77¬87.

[19] D. R. Harries, Irradiation creep in non-fissile metals and alloys, Journal of Nuclear Materials, 65 (1977) 157–173.
[20] W. Schüle, H. Hausen, Neutron irradiation creep in stainless steel alloys, Journal of Nuclear Materials, 212–215 – P1 (1994) 388–392.
[21] E. R. Gilbert, J. F. Bates, Dependence of irradiation creep on temperature and atom displacements in 20% cold-worked type 316 stainless steel, Journal of Nuclear Materials, 65 (1977) 204–209.
[22] J. Garnier, et al., Irradiation creep of SA 304L and CW 316 stainless steels: Mechanical behavior and microstructural aspects. Part I: Experimental results, Journal of Nuclear Materials, 413 (2011) 63–69.
[23] G. W. Lewthwaite, The acceleration of climb-controlled creep by neutron irradiation, Journal of Nuclear Materials, 38 (1971) 118–120.
[24] P. T. Heald, M. V. Speight, Steady-state irradiation creep, Philosophical Magazine, 29 (1974) 1075–1080.
[25] R. V. Hesketh, A transient irradiation creep in non-fissile metals, Philosophical Magazine, 8 (1963) 1321-1333.
[26] G. W. Lewthwaite, K. J. Proctor, Irradiation-creep in a materials testing reactor, Journal of Nuclear Materials, 46 (1973) 9–22.
[27] J. R. Matthews, M. W. Finnis, Irradiation creep models – an overview, Journal of Nuclear Materials, 159 (1988) 257–285.
[28] F. A. Garner, D. S. Gelles, Irradiation Creep Mechanisms: An Experimental Perspective, Journal of Nuclear Materials, 159 (1988) 286-309.
[29] L. K. Mansur, Irradiation creep by climb-enabled glide of dislocations resulting from preferred absorption of point defects, Philosophical Magazine A, 39 (1979) 497-506.
[30] V. I. Dubinko, New mechanism of irradiation creep based on the radiation-induced vacancy emission from dislocations, Radiation Effects and Defects in Solids: Incorporating Plasma Science and Plasma Technology, 160 (2005) 85–97.
[31] D. A. Vermilyea, A theory for the propagation of stress corrosion cracks in metals, Journal of Electrochemical Society, 119 (1972) 405–407.
[32] ASTM, Stress Corrosion Cracking — The Slow Strain-rate Technique, ASTM STP 665, Eds.: G. M. Ugiansky and J. H. Payer, American Society for Testing and Materials, Philadelphia, PA, 1979.
[33] J. C. Scully, The interaction of strain-rate and re-passivation rate in stress corrosion crack propagation, Corrosion Science, 20 (1980) 997–1016.
[34] R. N. Parkins, 1990 Plenary Lecture: Strain rate effects in stress corrosion cracking, Corrosion, 46 (1990) 178-189.
[35] ASTM, Slow Strain Rate Testing for the Evaluation of Environmentally Induced Cracking: Research and Engineering Applications, ASTM STP 1210, American Society for Testing and Materials, Philadelphia, PA, 1993.
[36] F. P. Ford, Mechanisms of Environmental Cracking in Systems Peculiar to the Power Generating Industry, EPRI NP-2589, Electric Power Research Institute, Palo Alto, CA, September 1982.
[37] ASTM, Standard Practice for Slow Strain Rate Testing to Evaluate the Susceptibility of Metallic Materials to Environmentally Assisted Cracking, ASTM G129–00, American Society for Testing and Materials, West Conshohocken, PA, November 2000.
[38] Y. S. Garud, T. L. Gerber, An engineering model for predicting stress corrosion cracking, in: Advances in Life Prediction, Eds.: D. A. Woodford and J. R. Whitehead, The American Society of Mechanical Engineers, New York, NY, 1983, pp. 75–83.
[39] Y. S. Garud, Development of a Model for Predicting IGSCC of Alloy 600 in PWR Primary Water, EPRI NP-3791, Electric Power Research Institute, Palo Alto, CA, January 1985.
[40] J. M. Boursier, et al., Stress corrosion cracking of Alloy 600 water: influence of strain rate on different stages of cracking, in: EUROCORR'92, Vol. II, Espoo, 1992, pp. 11–19.
[41] H. Takaku, M. Tokiwai, H. Hirano, Effects of cyclic tensile loading on stress corrosion cracking susceptibility for sensitized Type 304 stainless steel in 290 C high purity water, Corrosion, 35 (1979) 523–531.
[42] T. S. Bulischeck, D. van Rooyen, Stress corrosion cracking of Alloy 600 using the constant strain rate test, Corrosion, 37 (1981) 597–607.
[43] D. van Rooyen, Stress Corrosion Cracking of PWR Steam Generator Tubing, BNL-NUREG-51454, Vol. 1, No. 4, February 1982.
[44] R. Bandy, D. van Rooyen, Quantitative Examination of Stress Corrosion Cracking of Alloy 600 in High Temperature Water—Work During 1983, Brookhaven National Laboratory, Upton, NY, 1983.
[45] M. Hishida, H. Nakada, Constant strain rate testing of Type 304 stainless steel in high temperature water—Part I: Evaluation of stress corrosion cracking susceptibility, Corrosion, 33 (1977) 332–338.
[46] W. L. Clarke, G. M. Gordon, Investigation of stress corrosion cracking susceptibility of Fe-Cr-Ni alloys in nuclear reactor water environments, Corrosion, 29 (1973) 1–12.
[47] J. K. Sung, G. S. Was, Intergranular cracking of Ni-16Cr-9Fe Alloys in high temperature water, Corrosion, 47 (1991) 824–834.
[48] G. S. Was, J. K. Sung, T. M. Angeliu, Effects of grain boundary chemistry on the intergranular cracking behavior of Ni-16Cr-9Fe in high-temperature water, Metallurgical Transactions A, 23A (1992) 3343–3359.
[49] T. M. Angeliu, G. S. Was, Creep and intergranular cracking of Ni-Cr-Fe-C in 360 °C Argon, Metallurgical Transactions A, 25A (1994) 1169–1183.
[50] W. Kuang, G. S. Was, The effects of grain boundary carbide density and strain rate on the stress corrosion cracking behavior of cold rolled Alloy 690, Corrosion Science, http://dx.doi.org/10.1016/j.corsci.2015.04.020.
[51] A. Oehlert, A. Atrens, Primary creep and stress corrosion cracking, in: Parkins Symposium on fundamental aspects of stress corrosion cracking, Eds: S. M. Bruemmer, E. I. Meletis, R. H. Jones, W. W. Gerberich, F. P. Ford, and R. W. Staehle, The Minerals, Metals and Materials Society, Warrendale, PA, 1992, pp. 255–275.
[52] K. van Gelder, et al., The stress corrosion cracking of duplex stainless steel in H2S/CO2/CL− environments, Corrosion Science, 27 (1987) 1271–1279.
[53] R. N. Iyer, R. F. Hehemann, Strain-rate effects in hydrogen embrittlement of a ferritic stainless steel, in: Environment-induced Cracking of Metals (NACE-10), Eds.: R. P. Gangloff and M. B. Ives, NACE, Houston, TX, 1990, pp. 527–530.
[54] H. Leinonen, Stress corrosion cracking and life prediction evaluation of austenitic stainless steels in calcium chloride solution, Corrosion, 52 (1996) 337–346.

[55] D. G. Eisenhut, B. D. Liaw, J. Strosnider, Summary of Operating Experience with Recirculating Steam Generators, NUREG-0523, U.S. Nuclear Regulatory Commission, Washington, D. C., January 1979.
[56] R. N. Duncan, et al., Stainless-steel-clad fuel rod failures, Nuclear Technology, 1 (1965) 413–418.
[57] Y. S. Garud, An incremental damage formulation for stress corrosion cracking and its application to crack growth interpretation based on CERT data, Corrosion, 46 (1990) 968-974.
[58] S. R. Bodner, Y. Partom, Constitutive equations for elastic-viscoplastic strain-hardening materials, Journal of Applied Mechanics, Transactions of the ASME, 42 (1975) 385–389.
[59] R. S. Treseder, R. P. Badrak, Effect of cold-working on SCC resistance of carbon and low alloy steels – A review, Corrosion'97, Paper No. 41, NACE, Houston, TX, 1997.
[60] Y. S. Garud, G. O. Ilevbare, An SCC initiation model: Effects of cold-cork in austenitic stainless steels in light water reactor environment, International Journal of Nuclear Energy Science and Engineering, 2 (2012) 79–87.
[61] D. van Rooyen, Stress Corrosion cracking of PWR Steam Generator Tubing, in BNL-NUREG-51454, Vol. 1, No. 3, November 1981.
[62] T. S. Bulischeck, D. van Rooyen, Effect of environmental variables on the stress corrosion cracking of Inconel 600 steam generator tubing, Nuclear Technology, 55 (1981) 383–393.
[63] J. R. Scully, P. J. Moran, Influence of strain on the environmental hydrogen assisted cracking of a high-strength steel in sodium chloride solution, Corrosion, 44 (1988) 176–185.
[64] C. H. Shen, P. G. Shewmon, Mechanism of hydrogen-induced intergranular stress corrosion cracking in Alloy 600, Metallurgical Transactions, 21A (1990) 1261–1271.
[65] H. S. da Costa-Mattos, I. N. Bastos, J. A. C. P. Gomes, A simple model for slow strain rate and constant load corrosion tests of austenitic stainless steel in acid aqueous solution containing sodium chloride, Corrosion Science, 50 (2008) 2858–2866.
[66] F. Q. Yang, et al., A quantitative prediction model of SCC rate for nuclear structure materials in high temperature water based on crack tip creep strain rate, Nuclear Engineering and Design, 278 (2014) 686–692.
[67] S. A. Serebrinsky, J. R. Galvele, Effect of the strain rate on stress corrosion crack velocities in face-centered cubic alloys: A mechanistic interpretation, Corrosion Science, 46 (2004) 591–612.